

Probing kinetically excited hot electrons using Schottky diodes

Dhruva D. Kulkarni and Daniel A. FieldDaniel B. CutshallJames E. HarrissWilliam R. HarrellChad E. Sosolik

Citation: *Journal of Vacuum Science & Technology B, Nanotechnology and Microelectronics: Materials, Processing, Measurement, and Phenomena* **35**, 03D103 (2017); doi: 10.1116/1.4979003

View online: <http://dx.doi.org/10.1116/1.4979003>

View Table of Contents: <http://avs.scitation.org/toc/jvb/35/3>

Published by the [American Vacuum Society](#)

Articles you may be interested in

[Interaction study of nitrogen ion beam with silicon](#)

Journal of Vacuum Science & Technology B, Nanotechnology and Microelectronics: Materials, Processing, Measurement, and Phenomena **35**, 03D101 (2017); 10.1116/1.4977566

[Creating and probing quantum dot molecules with the scanning tunneling microscope](#)

Journal of Vacuum Science & Technology B, Nanotechnology and Microelectronics: Materials, Processing, Measurement, and Phenomena **35**, 04F102 (2017); 10.1116/1.4979848

[X-ray analysis of metamorphic \$\text{In}_x\text{Ga}_{1-x}\text{As}/\text{In}_y\text{Ga}_{1-y}\text{As}\$ superlattices on GaAs \(001\) substrates](#)

Journal of Vacuum Science & Technology B, Nanotechnology and Microelectronics: Materials, Processing, Measurement, and Phenomena **35**, 03D105 (2017); 10.1116/1.4979323

[Exploring the fabrication of Co and Mn nanostructures with focused soft x-ray beam induced deposition](#)

Journal of Vacuum Science & Technology B, Nanotechnology and Microelectronics: Materials, Processing, Measurement, and Phenomena **35**, 031601 (2017); 10.1116/1.4979274

[Electrical and optical characteristics of gamma-ray irradiated AlGaIn/GaN high electron mobility transistors](#)

Journal of Vacuum Science & Technology B, Nanotechnology and Microelectronics: Materials, Processing, Measurement, and Phenomena **35**, 03D107 (2017); 10.1116/1.4979976

[Study of device instability of bottom-gate ZnO transistors with sol-gel derived channel layers](#)

Journal of Vacuum Science & Technology B, Nanotechnology and Microelectronics: Materials, Processing, Measurement, and Phenomena **35**, 03D104 (2017); 10.1116/1.4979321



Probing kinetically excited hot electrons using Schottky diodes

Dhruva D. Kulkarni and Daniel A. Field

Department of Physics and Astronomy, Clemson University, Clemson, South Carolina 29634

Daniel B. Cutshall

Holcombe Department of Electrical and Computer Engineering, Clemson University, Clemson, South Carolina 29634

James E. Harriss

Department of Physics and Astronomy, Clemson University, Clemson, South Carolina 29634

William R. Harrell

Holcombe Department of Electrical and Computer Engineering, Clemson University, Clemson, South Carolina 29634

Chad E. Sosolik^{a)}

Department of Physics and Astronomy, Clemson University, Clemson, South Carolina 29634

(Received 30 December 2016; accepted 28 February 2017; published 28 March 2017)

Hot electron generation was measured under the impact of energetic Ar and Rb ions on Ag thin film Schottky diodes. The energy- and angular-dependence of the current measured at the backside of the device due to ion bombardment at the frontside is reported. A sharp upturn in the energy dependent yield is consistent with a kinetic emission model for electronic excitations utilizing the device Schottky barrier as determined from current–voltage characteristics. Backside currents measured for ion incident angles of $\pm 30^\circ$ are strongly peaked about 0° (normal incidence) and resemble results seen in other contexts, e.g., ballistic electron emission microscopy. Accounting for the increased transport distance for excited charges at non-normal incidence, the angular results are consistent with the accepted mean free path for electrons in Ag films. © 2017 American Vacuum Society.

[<http://dx.doi.org/10.1116/1.4979003>]

I. INTRODUCTION

In exothermic gas interactions at metal surfaces the dissipation of energy into the nuclear and electronic degrees of freedom of the metal typically occurs through the excitation of photons, phonons, or electrons. Of these energy loss channels, the most difficult to detect experimentally has been the excitation of electron-hole pairs. Using Schottky diode gas sensing devices, Nienhaus and others have performed measurements which give clear evidence for the electron–hole pair excitation channel under thermal energy gas exposure.^{1,2} While their results indicate that electron–hole pair excitations are a common avenue for energy loss during a gas–surface interaction at thermal energies, there have been few studies that measure the role of this channel for higher energy projectiles.

One of the first experimental demonstrations of electron–hole pair detection in energetic beam scattering was the work of Amirav and Cardillo who were able to measure excitations at Ge(100) and InP(100) surfaces under Xe exposure.^{3,4} Using neutral Xe, with incident energies of 1–10 eV, a transient excitation current was seen upon impact that appeared to coincide with the creation of a local thermal “hot spot” at the surface. Other works have focused on metals and device-based measurements, such as the metal-oxide-semiconductor (MOS) results of Ref. 5 and the metal-insulator-metal (MIM) results of Ref. 6. The MOS measurements showed a velocity-dependence that was below the so-called classical threshold

for excitation of hot carriers over the internal barrier height of the device while the MIM data showed an energy-dependence which appeared to saturate at low incident energies (5–6 keV). In both cases, the detected hot carrier currents were required to overcome the tunnel barriers imposed by the buried insulating layers of the devices. In the work presented here, we revisit the problem of hot carrier generation using devices with no insulating barrier (Schottky diodes), measuring device currents generated as a function of the incident ion energy and angle.

In Sec. II, we present the details of our experiment including our Schottky device design. In Sec. III, we discuss the results of our measurements for Ar and Rb ions taken as a function of the ion energy and angle, respectively. A summary is presented in Sec. IV.

II. EXPERIMENT

The Schottky diodes used in these measurements were fabricated in-house at Clemson University. Silicon wafers (phosphorus doped Si (111)) with resistivities of $4.0 \pm 0.6 \Omega \text{ cm}$ (Monsanto, Inc.) served as substrates for the diodes. To form backside contacts, the wafers were etched with diluted hydrofluoric acid (2%) to remove native oxide and then $0.5 \mu\text{m}$ of Al was deposited and sintered at 450°C for 45 min in a nitrogen environment. Front-side rectifying contacts were deposited by thermal evaporation in the shape of a 6 mm dot of 99.999% Ag, as shown in Fig. 1(a). The thickness of the Ag dot was chosen to be 25 nm as discussed below. Figure 1(b) shows current–voltage (I–V) characteristics typical of

^{a)}Electronic mail: sosolik@clemson.edu

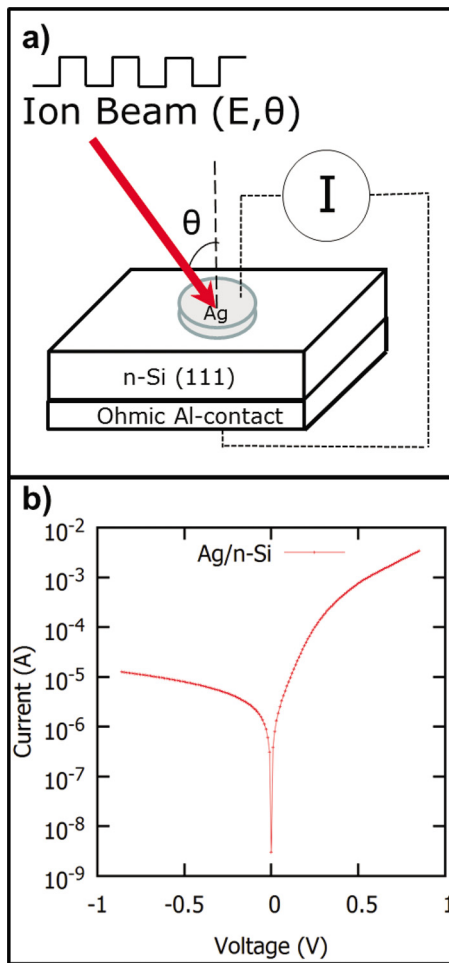


FIG. 1. (Color online) (a) Schematic representation of the Schottky diode (25 nm Ag/n-Si) irradiated by a pulsed ion beam with varying kinetic energy and angle of incidence. Current through the device is measured using a Keithley 617 picoammeter. (b) Current–voltage characteristics of a typical Schottky diode used in these measurements. A barrier height of 0.83 eV and an ideality factor of 1.9 are representative of the parameters for the diodes fabricated for this experiment.

one of our fabricated diodes. Ideality factors of ~ 1.9 and barrier heights of ~ 0.83 eV were obtained for the diodes, which is similar to the characteristics of Schottky diodes used in previous studies.² For *in situ* measurements, electrical contacts to the front-side were made using conductive silver paste (Ted Pella, Inc.).⁷

The ion beam irradiations of fabricated devices were performed using the singly charged ion beamline at Clemson University.⁸ Beams were incident on the front-side Ag contact of each device, and the resulting current through the device was measured using a Keithley 617 picoammeter connected as shown in Fig. 1(a). This current was measured as a function of two beam parameters: kinetic energy and angle of incidence. The kinetic energy was varied from 500 to 1500 eV at normal incidence. The angle of incidence was varied from -60° to $+60^\circ$ at a fixed kinetic energy of 5 keV.

The kinetic energy dependent measurements were performed using Rb^+ ions in a five-port custom vacuum chamber mounted directly in front of an aluminosilicate emitter ion source obtained from Heatwave Tech.⁹ The energy spread of

the beam was less than 1%. The setup is shown schematically in Fig. 2 where the ion beam was directed along the Z-axis while the device could be translated along the X-axis. The beam passed through a metal capillary (diameter 2.3 mm) mounted on a wide metal plate (width 25.4 mm) before reaching the diode surface. The capillary served as a mask to ensure that the ion beam interacted only with the top rectifying contact. The capillary was mounted on a translator parallel to the Y-axis, placing it ~ 5 mm from the device surface. Beam transmission through the metal capillary was measured previously and is detailed elsewhere.¹⁰ A Faraday cup in plane with the sample (not shown in the schematic) was used for beam tuning and for measuring ion beam currents pre- and postexposure. As the devices used in this experiment were photosensitive, care was taken to cover all vacuum port windows and limit signals arising from external light sources. However, a direct line-of-sight with the filament producing the ion beam led to a background signal. To measure the response of the sample separated from the background, the ion beams were pulsed in front of the devices using in-path deflectors resulting in a time-dependent current response such as that shown in Fig. 3. The difference between the signal with the ion beam incident on the device and the background level was determined to be the current response to the ion beam.

Angular-dependent measurements were performed on a device mounted in the beamline scattering chamber using Ar^+ ions from a sputter ion source (Scienta Omicron

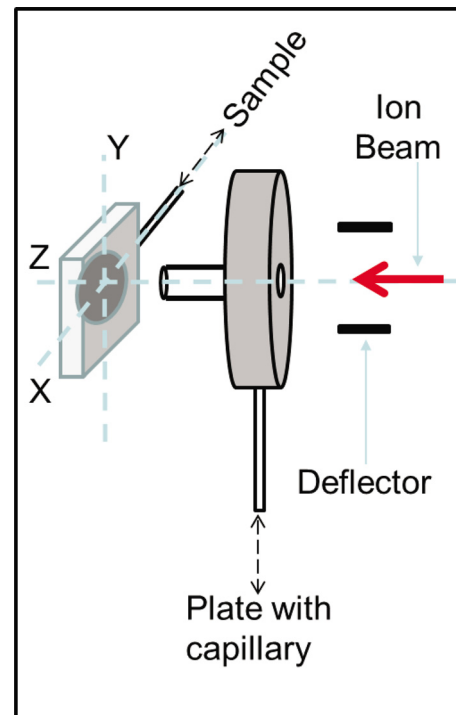


FIG. 2. (Color online) Schematic representation of the experimental setup used to conduct the ion irradiations. The energy dependence was measured in a custom vacuum chamber inserted into the beamline directly in front of the ion source. The capillary and the sample were translatable in the X and Y directions, respectively, as indicated. The in-path deflectors were used to pulse the ion beam to measure the response of the sample to the incident beam.

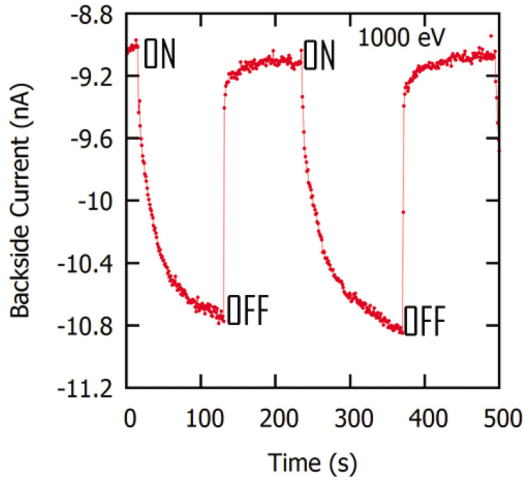


FIG. 3. (Color online) Hot electron current measured through a fabricated device in response to a pulsed Rb^+ beam at a kinetic energy of 1000 eV. The label ON signifies that the beam was directed onto the device face (e.g., at $t \approx 10$ s), while OFF signifies it was deflected away from the device face (e.g., at $t \approx 130$ s). The background signal when the beam is OFF is approximately -9 nA, while the measured signal is approximately -10.8 nA when the beam is ON.

ISE-10).¹¹ Here, a six-axis manipulator was used to position the device in the beam path, and the angle of incidence was varied by rotating the sample with respect to the incident beam axis.

One important parameter for these measurements was the thickness of the rectifying contact. First, a lower limit was placed on the metal contact thickness such that it would be greater than the penetration depth of the incident ions and avoid confounding our interpretation of hot electron current measurements. The software SRIM (Ref.12) was used to obtain penetration depths for our range of incident kinetic energies and a lower limit of 20 nm was obtained for the Ag film. An upper limit on the film thickness was set by considering the attenuation of any hot electron current by scattering events. It has been shown previously that the current attenuation inside a metal film depends exponentially on the film thickness (d) according to Beer's law²

$$I \propto I_0 \exp\left(\frac{-d}{\lambda_{\text{mfp}}(E) \cos(\theta)}\right), \quad (1)$$

where the nonscattered current, I , depends on the incident current, I_0 , which is attenuated exponentially according to the mean free path, $\lambda_{\text{mfp}}(E)$, for electrons in the film and the path length, $d/\cos(\theta)$, of those electrons through the film. The hot electrons are considered to undergo inelastic scattering events both with other cold electrons and the phononic system of the metal film, and both processes have a dependence on the excess energy of the hot electrons, hence the explicit energy dependence shown. The mean free path can also depend on the concentration of defects in the metal film. Estimates for the ballistic λ_{mfp} for polycrystalline metal films [see, e.g., Refs. 2, 13, and 14] find them to be tens of nanometers with values that vary depending on the technique used for measurement and on the quality of the film. Here,

we chose the thickness of our rectifying contact to be ~ 25 nm, within 5 nm of the lower limit and no more than a factor of two from typical λ_{mfp} values.

III. RESULTS AND DISCUSSION

A typical measurement of the current response of our fabricated Schottky diodes to a pulsed beam of Rb^+ ions is shown in Fig. 3 for a kinetic energy of 1000 eV. In Fig. 3, the label ON signifies that the beam was directed onto the device face (e.g., at $t \approx 10$ s), while OFF signifies it was deflected away from the device face (e.g., at $t \approx 130$ s). The background signal when the beam is OFF is approximately -9 nA, while the measured signal is approximately -10.8 nA when the beam is ON. As noted in Sec. II, the background signal in these data is attributed to the photosensitivity of the devices. For all measurements, the beam was directed onto the sample for a period of ~ 120 s, and the negative currents observed were consistent with electrons moving from the top Ag contact to the backside Al contact over the Schottky barrier. This direction of current flow is also consistent with previous measurements.^{1,2,5,6,15} To obtain a value for the hot electron current generated, we subtracted the response of the device from the baseline background signal. For the data shown in Fig. 3, the response was approximately -1.8 nA. The negative sign in the measured response is consistent with electron flow from metal to the semiconductor. As mentioned in Sec. II, the thickness of the metal film was chosen such that the incident ions would not have sufficient kinetic energy to reach the metal–semiconductor interface and thus the signal measured at the backside is not confounded by the ion current. We note that the additional time dependence observed within each time pulse is due to a capacitive effect from the deflectors used to deflect the beam. A similar time dependence was observed in beam currents measured using the in-plane Faraday cup.

Similar data were taken at other kinetic energies between 500 and 1500 eV in steps of 250 eV. For each measurement, the ion current incident onto the sample face was recorded and used to normalize the measured response and obtain the hot electron yield as a function of kinetic energy, as shown in Fig. 4. The error bars are drawn taking into account a 50 pA variation in 1 nA (5%) in the measured currents. We find no appreciable increase in the yield data for energies below 1000 eV, while a significant increase is observed at higher energies. This upturn can be interpreted as a threshold for hot electron production and detection for ions of ~ 1000 eV.

Typically, for exoelectron emission, a threshold is observed within the “kinetic electron excitation” (KEE) model,⁵ which can be thought of as an ion-analog for the photoelectric effect where electron emission from a metal surface into the vacuum arises due to ion bombardment instead of photon bombardment. In the KEE model, the metal surface is idealized as a Fermi gas, and a threshold ion velocity (v_{th}) for exoelectron emission, analogous to the photon frequency in the photoelectric effect, is calculated taking into account energy transfer to the electronic system of the metal by binary collisions and the depth of the potential

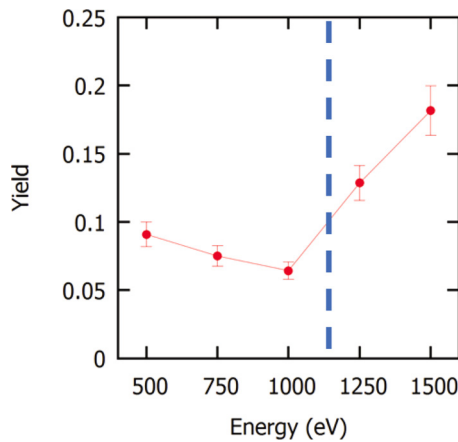


FIG. 4. (Color online) Yield of hot electrons plotted as a function of the kinetic energy of the incident ions. The dashed blue line at 1139 eV represents a threshold energy calculated for Rb^+ ions on a Ag film using a KEE model [Eq. (2)]. See text for details.

barrier trapping the excited electrons. We can apply the KEE model [Eq. (2)] to the case of hot electron current in the Schottky diode by substituting for the potential barrier the device Schottky barrier height $\phi_b = 0.83$ eV along with Fermi energy E_f and Fermi velocity v_f for our Ag film, 5.49 eV and 1.39×10^6 m/s, respectively, giving a threshold velocity $v_{th} = 5.06 \times 10^4$ m/s

$$v_{th} = 0.5 v_f \left[\sqrt{1 + (\phi_b/E_f) - 1} \right]. \quad (2)$$

For the ion species used in our experiment (Rb^+), the calculated threshold velocity corresponds to a kinetic energy of 1139 eV, which is represented as the dashed vertical blue line in Fig. 4. This threshold value agrees well with the upturn observed in our data near 1000 eV.

The incident angular dependence of the hot electron generation, measured for Ar^+ ions at a fixed kinetic energy of 5 keV, is shown in Fig. 5. We were constrained to an energy of 5 keV

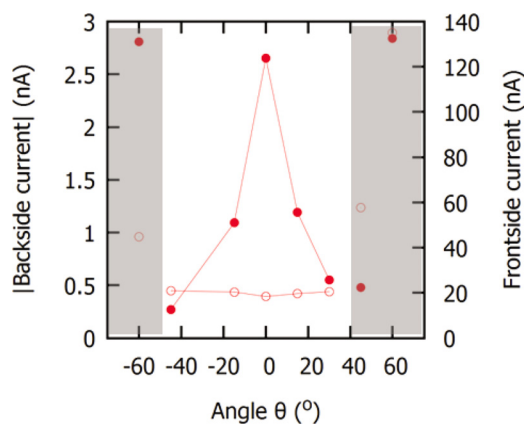


FIG. 5. (Color online) Variation in hot electron current as a function of the angle of incidence of a 5 keV Ar^+ beam. The frontside ion current represented by red open circles is approximately constant while the absolute value of the backside hot electron current represented by filled red circles is strongly peaked about the normal. The shaded areas correspond to regions where the signal is confounded with ion current and is disregarded. See text for details.

by the experimental setup for these measurements. For angles within the range $-45^\circ \leq \theta \leq 30^\circ$, we consider that the ion beam was directed fully onto the sample face, which is consistent with the constant front-side current observed in this range. As above, the hot electron current measured at the backside was negative in polarity and consistent with the data shown in Figs. 3 and 4. The absolute value of the hot electron current is plotted in Fig. 5 as a function of the angle of incidence. The yield at normal incidence is of the same order of magnitude as compared to the energy measurements. This current is strongly peaked about the normal incidence direction and falls off on either side monotonically. We note that as the device was rotated with respect to the incoming ion beam for angles beyond the range $-45^\circ \leq \theta \leq 30^\circ$, ions made contact with exposed wires. Therefore, data within these angular ranges (indicated by the shaded areas) are ignored in our analysis.

To understand the angular data, we note that as the angle of incidence is increased, the path length for the generated hot electrons to reach the Schottky barrier increases as $\cos^{-1}(\theta)$, as shown in Eq. (1). In Fig. 6, we plot the negative of the logarithm of the ratio of the normalized hot electron current measured at each angle θ to the normalized hot electron current measured at normal incidence versus the inverse of the cosine of the angle of incidence. If we interpret these data according to Eq. (1), the slope of the resulting line is the ratio of the film thickness to the mean free path of the hot electrons in the Ag film. The linear fit shown gives a slope of 4.8 ± 1.3 which, given that $d = 25$ nm, corresponds to a mean free path of 5.2 ± 1.4 nm. This mean free path value compares well with a value of 4.5 ± 0.5 nm previously reported from a hot electron current attenuation measurement conducted using Schottky diodes of varying Ag film thicknesses (p. 45 in Ref. 2). However, these values are lower than the values reported in the literature for MFP using other techniques, which could be attributed to the presence of a higher number of defects in the metal film.

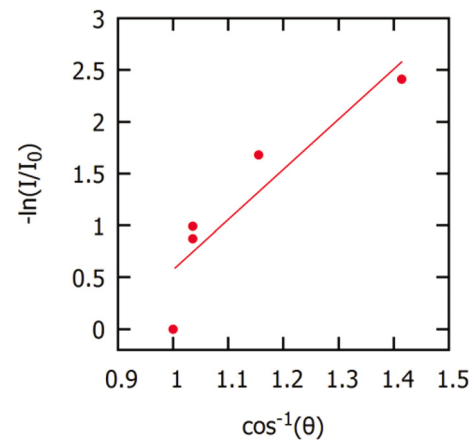


FIG. 6. (Color online) Figure illustrating the relation between the detected hot electron current and path length as given by Eq. (1). The ordinate is the negative of the logarithm of the ratio of the normalized hot electron current detected at an angle θ to the normalized hot electron current detected at normal incidence ($\theta = 0^\circ$), while the abscissa is the inverse of the cosine of the angle. The slope (4.8 ± 1.3), obtained from the linear fit, is the ratio of the film thickness to the mean free path of electron inside the film.

Ballistic electron emission microscopy (BEEM), a technique developed by Bell and Kaiser,^{16–18} can also be used to probe the directional momentum of hot electrons in a Schottky diode and as such is relevant to the angular measurements here. In BEEM, hot electrons from a negatively biased STM tip are injected into a metal surface and are collected, usually at a semiconductor interface, after passing through a Schottky barrier. The hot electron current is observed after a certain threshold bias voltage is reached. The transport of these hot electrons and their scattering within the metal film and at the metal–semiconductor interface is nontrivial. However, if we focus on our angular-dependent measurements, it is worth noting that in BEEM, using concepts of momentum conservation across the metal–semiconductor interface, there is a critical angle for the direction of the momentum of the hot electrons at the interface.^{19,20} Beyond this angle, hot electrons are reflected back into the metal surface instead of passing into the semiconductor, in analogy to total internal reflection of light. These reflected electrons can also undergo multiple reflections in the metal film, depending on its thickness, which can lead to randomization of the original direction and loss of directional information. While further analysis of our method is required before we can compare our measurements directly to such BEEM results, we note that this added angular dependence may serve as an additional factor suppressing the apparent mean free path for electrons in our Ag film.

IV. SUMMARY

We have fabricated Schottky diodes using 25 nm Ag films deposited onto n-type Si substrates and irradiated the top metal contacts with Rb⁺ and Ar⁺ ion beams of varying kinetic energy and angle of incidence, respectively. The kinetic energy was varied between 500 and 1500 eV, and a threshold for hot electron current detection was observed between 1000 and 1250 eV. A kinetic electron emission model applied to the subsurface Schottky barrier resulted in a calculated threshold value of 1139 eV, in good agreement with our observations. The angular dependent measurements suggest that there is an anisotropic generation and transport of hot electrons through the Ag film as there is a significant drop in the detected current for non-normal incident angles. Using these data and Beer's law, an estimate of the mean

free path for ballistic electrons in our Ag film is found to be 5.2 ± 1.4 nm. Defects in the metal film as well as nontrivial angular effects similar to those seen in BEEM measurements could contribute to this otherwise low λ_{mfp} value. We note that as the dependence of the observed hot electron current on the thickness of the metal film can be utilized to obtain the mean free path of hot electrons,^{21,22} measurements using diodes fabricated with metal films of varying thickness are currently underway.

ACKNOWLEDGMENTS

The authors gratefully acknowledge financial support from the National Science Foundation (NSF-DMR-0960100), DARPA (ARO Grant No. W911NF-13-1-0042), and the Clemson University College of Engineering, Computing and Applied Sciences.

¹B. Roldan Cuenya, H. Nienhaus, and E. W. McFarland, *Phys. Rev. B* **70**, 115322 (2004).

²H. Nienhaus, *Surf. Sci. Rep.* **45**, 1 (2002).

³A. Amirav, W. R. Lambert, M. J. Cardillo, P. L. Trevor, P. N. Luke, and E. E. Haller, *J. Appl. Phys.* **59**, 2213 (1986).

⁴A. Amirav and M. J. Cardillo, *Phys. Rev. Lett.* **57**, 2299 (1986).

⁵M. P. Ray, R. E. Lake, C. E. Sosolik, L. B. Thomsen, G. Nielsen, I. Chorkendorff, and O. Hansen, *Phys. Rev. B* **80**, 161405 (2009).

⁶S. Meyer, D. Diesing, and A. Wucher, *Phys. Rev. Lett.* **93**, 137601 (2004).

⁷Ted Pella, Inc., <http://www.tedpella.com/>.

⁸M. P. Ray, R. E. Lake, S. A. Moody, V. Magadala, and C. E. Sosolik, *Rev. Sci. Instrum.* **79**, 076106 (2008).

⁹Heat Wave Labs, Inc., <http://www.cathode.com/>.

¹⁰D. D. Kulkarni, L. A. M. Lyle, and C. E. Sosolik, *Nucl. Instrum. Methods* **382**, 54 (2016).

¹¹Scienta Omicron GmbH, <http://www.scientaomicron.com/>.

¹²J. F. Ziegler, J. P. Biersack, and U. Littmark, *The Stopping and Range of Ions in Matter* (Pergamon, New York, 1985).

¹³H. Kanter, *Phys. Rev. B* **1**, 522 (1970).

¹⁴C. R. Crowell and S. M. Sze, *Phys. Rev. Lett.* **15**, 659 (1965).

¹⁵S. Meyer, C. Heuser, D. Diesing, and A. Wucher, *Phys. Rev. B* **78**, 035428 (2008).

¹⁶W. J. Kaiser and L. D. Bell, *Phys. Rev. Lett.* **60**, 1406 (1988).

¹⁷W. J. Kaiser and L. D. Bell, *Annu. Rev. Mater. Sci.* **26**, 189 (1996).

¹⁸P. L. de Andres, F. J. Garcia-Vidal, K. Reuter, and F. Flores, *Prog. Surf. Sci.* **66**, 3 (2001).

¹⁹L. D. Bell, *Phys. Rev. Lett.* **77**, 3893 (1996).

²⁰L. D. Bell, *J. Vac. Sci. Technol., A* **15**, 1358 (1997).

²¹H. Lee, I. I. Nedrygailov, C. Lee, G. A. Somorjai, and J. Y. Park, *Angew. Chem. Int. Ed.* **54**, 2340 (2015).

²²I. I. Nedrygailov, C. Lee, S. Y. Moon, H. Lee, and J. Y. Park, *Angew. Chem. Int. Ed.* **55**, 10859 (2016).